A Self-Adaptive Risk-Based Optimization for a Multi-Carrier Energy Microgrid Incorporating Renewable Energy Sources, Energy Storage Systems, and Responsive Thermal, Cooling, and Electrical Demands

Mohamad Emadi[a], Hamid Reza Massrur[b,] *, Esmaeel RokRok[c], and Amin Samanfar[a]

[a] *Department of Electrical Engineering, Khorramabad Branch, Islamic Azad University, Khorramabad, Iran*

[b] *Electrical Engineering Department, Sharif University of Technology, Tehran, Iran*

[c] *Department of Electrical Engineering, Engineering Faculty, Lorestan University, Iran*

Abstract

The optimal daily operation of multi-energy microgrid (MEM) systems is a tremendous challenge due to the mutual impact of different energies, non-constant efficiency and partial loads of several internal equipment, various energy purchasing prices, and different energy demands at the MEM output. In addition, the uncertainties of various renewable energy sources, energy purchasing prices, and energy demands may create serious risks for the MEM's operating costs. This paper presents a comprehensive risk-based decision-making framework for MEMs to address the mentioned challenges. In the proposed framework, the effects of the responsibility of cooling, thermal and electrical energy demands, and different kinds of energy storage, particularly ice storage, as well as the integration of several renewable energy sources, are investigated. The well-known CVaR method and the 2*m*+1 Point Estimate Method (PEM), which is a fast uncertainty analysis method based on the Taylor series, are employed to evaluate the risks associated with the system uncertainties. Moreover, to solve the complex non-linear problem of risk-based daily scheduling of MEM, a new self-adaptive optimization method based on the Wavelet theory named Self-adaptive Modified Slime Mould Algorithm (SMSMA) is introduced to ensure moving toward the global optimum. The proposed risk-based framework is implemented on a MEM system.

Keywords: Demand Response; Energy Hub; Microgrid; Multi-Energy Generation System; Renewable Energy.

* Corresponding author. Hamid Reza Massrur, *E-mail address:* h.massrur@sharif.edu

Nomenclature

Parameters

a^{boil} b^{boil}	Partial boiler coefficients.
$a_{\square}^{chp}, b_{\square}^{chp}, c_{\square}^{chp}, d_1^{chp}, d_2^{chp}$	Partial CHP coefficients.
$\phi_{SOC,max}^{TSS}$	The maximum charging/discharging limits for the ramp value of the TSS unit (*KW*).
$P_{Ch/dch,max}^{ESS}$	The maximum charge/discharge limit of the ESS unit (*KW*).

Variables

$L_{e,in}^{t}/L_{h,in}^{t}/L_{g,in}^{t}$	Electrical/Thermal/Gas power exchange with upstream grid *(KW)/(KW)/ (m^3/hour).*
$L_{e,out}^{t}/L_{h,out}^{t}/L_{c,out}^{t}$	Electrical/Thermal/Cooling energy demand at the outside of the MEM (*KW*).
$\mathcal{P}_t^{wind}$	Available electrical power by wind turbine unit (*KW*).
$\mathcal{P}_t^{PV}$	Available electrical power by the solar unit (*KW*).
$\mathcal{P}_{ch/dch,t}^{ESS}$	The charge/discharge value by ESS unit (*KW*).
$\Phi_t^{Ecb}/\Phi_t^{Gcb}$	Amount of generated thermal power by the electrical/gas consumed boiler (*KW).*
$\varpi_E^t/\varpi_G^t/\varpi_H^t$	Electricity/Gas/Heat energy exchange price with upstream grid ($).

1. Introduction

The traditional power system consists of collaborating large-scale power units located in distant places from the load demands. These power systems are mainly managed by centralized operators and use fossil fuels as their primary source. When the electrical demands have been increased in power systems, these centralized power units result in higher greenhouse gas emissions, a higher level of power losses, and challenge creation for the system reliability. To overcome these important problems, distributed energy resources and microgrids incorporating renewable energy sources are employed [1]. Reference [2] investigates the use of a flexible solar panel for generating energy on curved surfaces. The research utilized the practical application of flexible solar energy conversion, incorporating

environmental assessment and techniques focused on pilot projects.

Recently, the demand for cooling, thermal, and electrical energies has increased manifold. With the advancement in poly-generation units such as Combined Cooling, Heat, and Power (CCHP) units, natural gas is utilized to simultaneously meet cooling, thermal and electrical demands in distribution systems. Incorporating the natural gas, cooling, thermal and electrical energies in the energy supply enhances the system's reliability and efficiency. Reference [3] examines a medium-term timeframe to explore the topic of the imminent future. In this context, the economic impacts and enhancement of a blend of natural gas and diesel fuel were analyzed. The research utilized two modeling approaches and a multi-criteria decision-making method to evaluate the operational characteristics and emissions of a dual-fuel engine running on diesel and gasoline. The study employed the response surface method to analyze three factors - injection angle, injection start time, and compression ratio to investigate pollution emissions. The energy hub is a new concept for utilizing multi-carrier energy systems that connects different energy carriers with each other. The Multi-Energy Microgrid (MEM) is an energy hub that consists of various energy storage units and energy conversion equipment to supply electrical, cooling, and thermal energy demands. Moreover, the microgrids are integrated with different renewable energy sources [4].

According to the US Department of Energy, approximately 35% of electricity consumption is in the construction and commercial sectors. Of this 35%, about 12% is dedicated to air cooling and conditioning systems [5]. To reduce electricity consumption, ice storage technology has recently been used to provide cooling loads. Ice storage technology transfers electrical loads from peak consumption to off-peak times [6]. Ice storage basically consists of a chiller and an ice tank. A chiller is used in ice-making conditions, and the created ice is stored in the tank, and stored ice is used during peak load times. This system is very effective in reducing peak electrical consumption. Therefore, the chiller is turned off during peak hours, and the stored ice supplies the required cooling load. Among the benefits of cooling ice storage, the following can be mentioned: 1) Transferring the chiller electricity consumption to off-peak hours, correcting the electricity load curve and reducing electricity consumption, 2) Reducing the capacity of chillers and cooling towers, reducing the volume of piping facilities, 3) Reducing electrical equipment and related costs, 4) Increase chiller efficiency due to changing their working hours to off-peak consumption hours with entire load operation, 5) Ideal for projects that require CCHP [7].

One of the critical issues influencing the secure utilization of MEM systems is the integration of these systems with

renewable energies. Analysis of such integrated MEM systems, along with renewable energies, is doubly complicated. This complexity is due to the power generation uncertainties of such renewable energy sources. On the other hand, in such systems, due to the existence of different energy loads, including electrical, cooling, thermal, or gas loads, there are uncertainties in the exact value determination of different types of system loads. Therefore, the existence of uncertainties in the MEM system may create serious risks for the microgrid operator [8]. In [9], the uncertainty of renewable energy sources and load demand forecasting for the unit of consumption are considered. Initially, real data is used to solve the non-homogeneous Markov model for the wind energy source and the homogeneous Markov model for the solar energy source. Subsequently, the microgrid system is implemented. However, the effects of different energy storage methods are not considered in this study.

There is valuable literature in the field of the optimal management of energy systems. When an energy system contains just one energy carrier, the optimal system operation is less complex as it does not take into account the interdependency between different forms of energy. In [10], an algorithm is investigated for the optimal scheduling of a grid-connected micro-grid, including a micro-turbine, a wind turbine, a diesel generator, a battery bank, and a fuel cell. In this work, the Genetic Algorithm (GA) is employed to perform the scheduling and economic optimization of the microgrid. In [11], a non-linear energy management strategy has been presented for a residential building with a battery bank and a rooftop photovoltaic system.

Gidel and et al. [12] were pioneers in introducing the definitions and concepts of the energy hub. In [13], the authors have presented a general energy flow model for multi-carrier energy systems such as integrated heat, natural gas, and electricity networks containing energy hubs. The optimal energy flow problem of a multi-carrier energy system with different renewable sources has been solved in [14,15]. Ref. [16] has investigated a multi-period optimization method to solve the energy dispatch problem of an energy hub considering biomass energy for heating. In [17,18], the purchasing/generation amount of each energy is determined and optimized according to the various load values and the prices of upstream energy carriers. In [19], a hierarchical energy management is developed for several home energy centers. The authors did not consider the system uncertainty; for example, the uncertainties of the output power of renewable-based DGs and electricity tariffs are not considered. In [20], taking into account the uncertainty of load demands, a new method for scheduling and optimal operation of energy hubs has been presented. However, the uncertainties of electricity prices have not been taken into account. Ref. [21] introduces an innovative approach to

tackle the uncertainties of integration of electric vehicles into the power grid by employing a non-stationary Markov chain. The application of a non-stationary discrete Markov model in this investigation offers a detailed and significant comprehension of the dynamic and time-varying characteristics of electric vehicle activities within the power grid. By conducting an in-depth case analysis, the results derived from the model provide compelling observations regarding the quantity of electric vehicles linked to the grid and the amount of energy they store throughout a 24-hour timeframe. Additionally, this study evaluates the precision of the model in depicting the load behavior of electric vehicle charging.

An integrated model for optimizing the operation and scheduling of energy hubs has been developed in [22], which considers the uncertainty of renewable DGs and the load demands of energy hubs. Ref. [23] presents the optimal stochastic scheduling of an energy hub considering the system's thermal and electrical energy markets. In this study, Monte Carlo simulation has been applied to investigate energy demands, wind power generation, and market price uncertainties. However, the Monte Carol simulation method has extreme computational complexity. Stochastic programming and Monte Carol simulation methods are widely used to evaluate the uncertainties of optimization problems. However, the main drawback of stochastic programming is that it imposes an enormous computational burden on problem-solving [24]-[25].

Demand response refers to the adjustment in electricity usage by customers of an electric utility in order to align power consumption with the available supply [26]. Reference [27] introduces a novel approach for regulating demand response involvement in load frequency control while accounting for communication time delays. The extended state observer is employed to estimate the level of Load Disturbance (LoD), taking into consideration the inherent uncertainty in power system parameters. Subsequently, the demand response program is integrated into load frequency control to offset either the entirety or a portion of the LoD, based on the power accessible at the aggregators and the communication time delay. However, the effects of other responsible loads in the system are not taken into account.

The authors in [28] have presented a stochastic model for a multi-carrier hub, in which the demand response capabilities of the hub, as well as the electricity and thermal energy markets, are considered. However, the effects of cooling and ice storage systems on the hub's operating costs are not investigated. The economic operation of a multi-carrier energy system using the connection matrix and the virtual nodes is proposed in [29]. Although this study has considered several energy sources and the responsibility effects of the demands, it did not study the effect of the cooling system and the modeling of partial loading of the equipment. In [30], multi-carrier microgrids that can

exchange energy with each other are investigated, but the effects of cooling systems and the responsibility effects of the demands are not discussed.

To reduce energy systems' operating costs, energy storage systems play an essential role in the system's operation. The energy storage systems increase the system's overall performance and flexibility. For example, an electric storage unit stores energy during periods of low electricity prices, and it will discharge during peak consumption hours [31]. An energy hub model is proposed in [32], which aims to maximize the benefit of the system. However, it does not consider cooling system modeling and demand response programs. In [33], a framework for participation in multi-carrier energy systems is presented, which integrates renewable energy sources and energy storage systems in the energy hub system. However, the responsible effects of cooling, thermal and electric demands, and ice storage effects on the systems have not been studied. Reference [34] introduces an enhanced framework for a MEM incorporating both electricity and natural gas, along with integrated solar, wind, and energy storage systems. The model, centered around energy hubs, is designed to reduce operational expenses and decrease greenhouse gas emissions. Reference [35] entails the execution of experiments and three-dimensional computational fluid dynamics analysis to investigate the heat transfer and fluid flow properties within an energy storage system of a solar air heater with a roughened wall. The roughened wall is characterized by a rectangular S-shaped pattern in two arrangements: staggered and inline. The thermal efficiency of the roughness design is a crucial aspect, with the orientation and shape of the irregularity playing a significant role. Nevertheless, the impact of this storage system has not been explored in the context of a multi-energy microgrid operation.

As can be seen from the literature review on the energy hubs, some significant aspects related to energy hubs have not yet reached maturity and development. Among the critical existing challenges that should be addressed more deeply than the previous research, we can point out the role of ice storage technologies in the optimal operation of energy hubs. Also, another remaining challenge that should be satisfactorily addressed is the investigation of the responsibility effects of thermal and cooling demands besides the electrical demand response. Notably, most of the previous studies have only assayed the effects of electrical demand response. In addition, using a fast analysis method to evaluate the energy hub system's uncertainties can increase the efficiency and speed of the hub's operation scheduling. Moreover, an appropriate tool must measure the risk associated with the hub's operating costs.

According to the mentioned topics, this paper presents a comprehensive risk-based framework for the probabilistic

scheduling of a MEM in the presence of responsive cooling, thermal, and electrical loads. In the modeling of MEMs, the effectiveness of the most important technologies, such as ice storage technology and Power to Gas (P2G) units [36], have been addressed. The risk-based framework uses the well-known Conditional Value at Risk (CVaR) approach and the 2*m*+1 Point Estimation Method (PEM), which can quickly analyze the uncertain variables based on the Taylor series to measure the risks pertaining to the MEM's operating costs. The 2*m*+1 PEM only utilizes the information on the skewness and kurtosis of the Probability Distribution Functions (PDF) and analyzes the system uncertainties with appropriate accuracy [37]. In this regard, various types of uncertainties are investigated, such as the uncertainties of cooling, thermal and electrical loads, renewable resources, and energy purchasing prices of upstream energy carriers. In this paper, the MEM's internal energy converters equipment is modeled as equipment with non-constant efficiency, and the effects of partial loading of equipment are considered using non-linear relationships. Table 1 presents the taxonomy of the proposed risk-based optimal decision-making compared to the state-of-the-art and the existing literature.

Numerical algorithms such as MILP have high speed in optimizing problems. However, they have poor performance when solving non-convex problems because these algorithms can easily be trapped in local optima in these conditions. On the other hand, meta-heuristic algorithms and evolutionary-based optimization approaches used in power systems are more efficient due to straightforward implementation and high efficiency [38]-[39]. For example, Particle Swarm Optimization (PSO) was employed for the optimal management of an integrated system, including wind units coupled with a battery [39]. Co-evolutionary PSO was applied to smart home operation strategies [40]. In Ref. [41], the optimal scheduling of a distribution network is acquired using a hybrid algorithm incorporating a bacterial foraging algorithm and PSO. Ref. [42] proposes the expansion planning problem of a single MEM with various energy sources using the PSO search algorithm. In [43], the slime mold algorithm is applied to solve the node-selecting approach for a traffic network problem. The Slime Mould Algorithm (SMA) is a novel population-based optimization method presented in 2020 by Mirjalili & et al that has more capability for solving many problems than the popular algorithms [44].

Notwithstanding high accuracy and ability compared with other algorithms, SMA has not yet been exerted to solve MEM scheduling problems. However, the original SMA in some optimization problems, is trapped in local optima

due to adjusting the exploration and exploitation process and high non-linearity environment of the problems. The main reason for this issue is that SMA's mutation mechanism, which causes varying solutions, is not effectively robust for all optimization problems. Therefore, to enhance the SMA's robust ability to move towards the global solution of energy management of MEMs, this paper presents a new self-adaptive modified technique for the original SMA based on the Wavelet theory. The effectiveness of the new self-adaptive modified SMA algorithm has been presented with numerical results in Section 5.

In summary, this paper develops a comprehensive risk-based framework for the stochastic scheduling of a MEM system with responsive cooling, thermal, and electrical loads. The modeling of MEMs incorporates key technologies such as P2G, Combined Heat and Power (CHP), various boilers, chillers, and different energy storage systems including Electrical Storage Systems (ESS), Heat Storage Systems (HSS), Gas Storage Systems (GSS), and Cooling Storage Systems (CSS). The framework utilizes the CVaR approach and the 2m+1 PEM to efficiently analyze uncertain variables. Various uncertainties are explored, including cooling, thermal, and electrical load uncertainties, uncertainties in renewable resources, and fluctuations in energy purchasing prices of upstream energy sources. The MEM's internal energy conversion equipment is modeled with non-constant efficiency, accounting for the effects of partial loading through non-linear relationships. Furthermore, a novel Self-adaptive modified Slime Mould is introduced to address the MEM's integrated non-convex and non-linear risk-based daily decision-making problem. In the following, the main contributions of this paper are expressed:

1) Developing a risk-based model for a multi-energy microgrid composed of P2G, CHP, various boilers, chillers, and different energy storage systems, including ESS, GSS, HSS, and CSS, and renewable energy sources. The comprehensive study of the storage system is an essential contribution of this paper compared to existing studies such as [17, 18], and [34]. In this paper, much attention has been paid to the ice storage systems to provide cooling if needed; Moreover, the impact of various responsive loads, such as electrical, heating, and cooling demands, on the total operating cost of a MEM system has been assessed.
2) Introducing a new Self-adaptive Modified SMA (SAMSMA) optimization algorithm to solve the integrated MEM's non-convex and non-linear risk-based daily decision-making problem.
3) The proposed framework considers vast areas of uncertainties including, PV and wind energy sources, various energy demands, and energy exchange prices with upstream energy networks.

4) Developing the MEM modeling utilizing non-constant efficiency and partial loads of the MEM's internal energy converter equipment.

The rest of this paper is formed as follows. In Section 2, the proposed integrated MEM structure is presented. Section 3 formulates the proposed risk-based daily scheduling framework of the integrated MEM. Section 4 represents the fast stochastic 2*m*+1 PEM uncertainty analysis method for solving the proposed optimization problem regarding the system uncertainties. The introduced SMSMA algorithm and its modification have been expressed in section 5. Section 6 investigates the performance of the proposed risk-based daily scheduling framework and the SMSMA algorithm with numerical results. In the end, Section 7 remarks on the paper's conclusions.

2. Proposed Multi-Energy Microgrid Structure

MEMs can be widely used for many purposes, including industrial, commercial, and residential applications [45]. Each MEM may contain three equipment types: energy conversion equipment, energy transmission units, and energy storage devices. Energy conversion equipment is required to convert energy carriers from one form to another. A general diagram of the MEM proposed in this paper is presented in Fig. 1. In this MEM, gas, heat, and electrical energies are the input energy sources, and electrical, heat, and cooling energies are the output demands. The input energies are converted or directly transported to the output point based on the MEM conditions and demands.

The electrical energy demand at the output of the MEM can be provided by the CHP, solar unit, wind power unit, or purchasing from the upstream network. To supply the thermal load at the output side of the MEM, the Gas-Consumed Boiler (GCB) or the Electric Boiler (EB) or generated thermal power by the CHP unit, as well as the purchased thermal power from the upstream network, can be utilized. Due to the price changes of electricity, thermal, and natural gas energies at the upstream networks during the daily operation of the MEM, the generated thermal power by the boiler, CHP, or the heat purchased from the upstream network can be stored in the Thermal Storage System (TSS). In addition, generated electric power by the CHP, solar unit, wind power unit, or purchased electric power from the upstream grid can be stored in the Electricity Storage System (ESS) during the day. Also, the required gas for gas-consuming units can be provided by purchasing from the upstream gas network and by using renewable energies and converting to gas by the P2G unit. Also, the gas in the MEM can be stored in the Gas Storage System

(GSS) for later hours.

To supply cooling loads, Absorption Chillers (AC) or Electric Chillers (EC) can be utilized. It is also possible to store the generated cooling power in the Ice Storage System (ISS) equipment. Ice storage-based air conditioning technology is the process of using ice to store thermal energy. This process can reduce the energy used for cooling during peak electrical demand. It uses standard cooling equipment, plus an energy storage tank to transfer all or part of the MEM's cooling needs to off-peak and nighttime hours. During off-peak hours, ice is made and stored in energy storage tanks. Notably, hydrogen systems are used for specific applications such as hydrogen-fueled vehicles or for specific utilities. Hence, since any hydrogen-consuming applications are not included in our model, we did not consider the water and hydrogen systems, power-to-hydrogen systems, or any related frameworks. Moreover, the process of producing hydrogen from water and using it for power generation is currently not cost-effective when the microgrid is equipped with CHP and the gas price is low. For this rational reason, we did not take into account the hydrogen-to-power system either.

The MEM is an independent entity that purchases different forms of energy from different upstream energy networks at a predetermined price to meet the MEM's output energy demand. The MEM operator can optimize the MEM's energy demands in response to variations in the input energy prices by changing the supplier energy at the MEM's input or changing the MEM's energy consumption pattern by employing demand response capability at the MEM's output. With the change in the supplier energy at the MEM input, the energy consumption does not change from the viewpoint of the responsive customers. However, the supplier energy source has been changed to another energy source. The MEM operators minimize their energy purchase costs by employing the flexibility achieved by converting heat, cold, gas, and electricity energies to each other. Therefore, the MEM operator can reduce the operating costs of the MEM by changing the consumption pattern of thermal, electrical, and cooling loads and employing the flexibility that results from the conversion of different energies to each other. Also, the MEM's storage units create an ability for the MEM to sell the MEM's surplus energy to upstream networks and reduce costs.

3. Mathematical Formulation of the Risk-Based MEM Energy Management Framework

The daily operation cost of the integrated MEM consists of the electrical, heat, and natural gas purchasing costs

from the upstream networks. The most critical issue that must be determined in the optimal daily operation of a MEM is the amount of converted energy by each internal equipment in the MEM and the amounts of exchanged energy with upstream networks, as well as storing energies in various storages. The operating costs of the integrated MEM should be minimized over the 24-hour horizon according to the following objective function:

$$Min(\mathrm{Cos}t_{MEM}) = \min\left[\sum_{t=1}^{24}(\varpi_E^t.L_{e,in}^t + \varpi_H^t L_{H,in}^t + \varpi_G^t.L_{G,in}^t + £_G.(F_t^{CHP} + F_t^{Gcb}\right] \quad (1)$$

where $£_G$ is the emission factors (per unit of gas energy) of cogeneration units. Eq. (1) represents the energy purchasing costs from the upstream networks as well as carbon production costs. This equation is based on the hourly reaction of the MEM against hourly energy prices considering environment costs. In Eq. (1), the uncertainties associated with the MEM system have not been taken into account, which can cause serious risks for the MEM operator. To make a trade-off between the MEM's operating costs and its pertaining risks, we consider the CVaR, which is a well-known tool for risk measurement. The CVaR value can be calculated for any given confidence level $\alpha \in [0, 1]$ as follows [46]:

$$CVaR = Min[\vartheta + \frac{1}{1-\alpha}\sum_{\rho\in \mathrm{P}} W_\rho.\max\{\mathrm{Cos}t_{hub,\rho} - \vartheta, 0\}] \quad (2)$$

where ϑ demonstrates VaR, ρ defines the sample point set in the $2m$+1 PEM method described in Section 4. $W\rho$ is the weighting factor corresponding to sample point ρ in the $2m$+1 PEM method. Hence, the MEM operator's objective function is to minimize the expected costs$(Cost_{hub})$, together with the weighted CVaR of the cost. Accordingly, Eq. (1) can be rewritten by the following equation:

$$Min[(1-\gamma)*\sum_{\rho=1}^{N_\rho} W_\rho.\mathrm{Cos}t_{hub,_\rho} + \gamma*(\vartheta + \frac{1}{1-\alpha}\sum_{\rho=1}^{N_\rho} W_\rho.\{\max(\mathrm{Cos}t_{hub,\rho} - \vartheta, 0)\})] \quad (3)$$

where $\Upsilon \in [0, 1]$ is a weighting factor that indicates the trade-off between the MEM's operating costs and its risks. The objective function (3) is constrained with Eqs. (4) - (47):

$$\mathrm{Cos}t_{hub,\rho} - \vartheta \le \Lambda_\rho, \forall\rho \in \mathrm{P} \quad (4)$$

$$\Lambda_\rho \ge 0, \forall\rho \in \mathrm{P} \quad (5)$$

where Λ_ρ is a positive auxiliary parameter that limits the difference between the operating costs corresponding to the

sample point ρ ($Cost_{hub,\rho}$) and the VaR value represented in Eq. (4).

This study focused on analyzing the optimal daily operation of a multi-energy microgrid from the perspective of microgrid operators. The investigation addressed various constraints relevant to microgrid operations. The microgrid operator needs to predict selling/purchasing wholesale market prices from/to upstream networks one day before the scheduling day. Although this prediction can be uncertain, it utilizes uncertainty analysis methods such as $2m$+1 PEM and CVaR method to mitigate their risks in the operations. Consequently, considering the power flow constraints of the upstream electricity network is unnecessary for the daily operation of the microgrid from the microgrid operator's perspective. Therefore, including electricity network constraints in the modeling or simulation results is considered irrelevant to the daily operation of the microgrid. Hence, the electricity network can be anything.

Eqs. (5) to (9) balance the electricity, gas, and heat energies at the input and output sides of the MEM, respectively:

$$L_{e,in}^{t} = P_{t}^{EC} + \mathrm{P}_{t}^{P2G} + P_{t}^{Ecb} + P_{ch,t}^{ESS} + L_{e,out}^{t} - \mathrm{P}_{t}^{CHP} - \mathrm{P}_{t}^{wind} - \mathrm{P}_{t}^{pv} - P_{dch,t}^{ESS} \tag{6}$$

$$L_{g,in}^{t} = \mathrm{F}_{t}^{Gcb} + \mathrm{F}_{t}^{CHP} + \mathrm{F}_{ch,t}^{GSS} - \mathrm{F}_{t}^{P2G} - \mathrm{F}_{dch,t}^{GSS} \tag{7}$$

$$L_{h,in}^{t} = \phi_{ch,t}^{CSS} + \phi_{t}^{AC} + L_{h,out}^{t} - \phi_{t}^{Ecb} - \phi_{t}^{Gcb} - \phi_{t}^{chp} - \phi_{dch,t}^{CSS} \tag{8}$$

$$\psi_{t}^{EC} + \psi_{t,c}^{AC} + \psi_{dch,t}^{ISS} = L_{c,out}^{t} + \psi_{ch,t}^{ISS} \tag{9}$$

where Φ_{t}^{CHP} and Φ_{t}^{boiler} are the generated heat power of CHP and boiler, respectively. F_{t}^{P2G} is the gas generation of the P2G unit. $\psi_{t}^{EC}$and $\psi_{t,C}^{AC}$ are the generated cooling energies by electrical and absorption chillers. According to the type of customers, electrical, thermal, and cooling energies at the output of the MEM are divided into two parts consisting of fixed and flexible loads as follows [47]:

$$L_{e,out}^{t} = L_{e,out,Fix}^{t} + L_{e,out,DR}^{t} \tag{10}$$

$$L_{h,out}^{t} = L_{h,out,Fix}^{t} + L_{h,out,DR}^{t} \tag{11}$$

$$L_{c,out}^{t} = L_{c,out,Fix}^{t} + L_{c,out,DR}^{t} \tag{12}$$

where $L_{e,out,Fix}^{t}$, $L_{h,out,Fix}^{t}$ and $L_{C,out,Fix}^{t}$ are the constant part of electrical, thermal, and cooling loads and $L_{e,out,DR}^{t}$, $L_{h,out,DR}^{t}$ and $L_{c,out,DR}^{t}$ are the responsible parts for electrical, thermal, and cooling loads. The total amount of electric, heat, and cooling loads for a day is fixed, and these loads can only be moved from one time period to another period

in the day. Therefore, the sum of electrical, thermal, and cooling loads every day must equal the following equations:

$$L_e^{day} = \sum_{t\in T} L_{e,out,Fix}^t + \sum_{t\in T} L_{e,out,DR}^t \tag{13}$$

$$L_h^{day} = \sum_{t\in T} L_{h,out,Fix}^t + \sum_{t\in T} L_{h,out,DR}^t \tag{14}$$

$$\psi_c^{day} = \sum_{t\in T} L_{c,out,Fix}^t + \sum_{t\in T} L_{c,out,DR}^t \tag{15}$$

The transfer percent of electric, thermal, and cooling loads per hour can only be equal to the responsibility percentage of the loads. Therefore, the following limit for the changes of responsive loads per hour should be observed:

$$L_{out,DR}^{t,\min} \le L_{out,DR}^t \le L_{out,DR}^{t,\max} \tag{16}$$

The following equation can be used to calculate the generated electrical power by the CHP unit (P_t^{chp}) [48]:

$$P_t^{chp} = \begin{cases} a^{chp}\phi_t^{chp} + b^{chp}T_{s,t}^{chp} + c^{chp} & for, d_1^{chp}\phi_t^{chp} \le \phi_t^{chp} \le \phi_H^{chp,\max} \\ a^{chp}\phi_t^{chp} + b^{chp}T_{s,t}^{chp} + c^{chp} - y_1^{chp} & for, d_2^{chp}\phi_H^{chp,\max} \le \phi_1^{chp}\phi_H^{chp,\max} \\ a^{chp}\phi_t^{chp} + b^{chp}T_{s,t}^{chp} + c^{chp} - y_1^{chp} - y_2^{chp} & for, \phi_H^{chp,\min} \le \phi_t^{chp} \le d_2^{chp}\phi_H^{chp,\max} \end{cases} \tag{17}$$

where P_t^{chp} is the electrical active power of CHP, and $\phi_{t,h}^{chp}$ is the CHP's generated thermal power. $\phi_{t,max}^{chp}$ and $\phi_{t,min}^{chp}$ are the minimum and maximum capacities of the CHP's output thermal power, respectively. The coefficients in Eq. (17) are constants and indicate the dependency between the production amount of CHP's thermal and electrical powers, known as the CHP's partial loading coefficients. T_s^{chp} is the CHP's temperature of the hot water. The parameters $d_{1,r}^{chp}$ and $d_{2,r}^{chp}$ are called loading constants and are obtained from the following relations:

$$d_{1,r}^{chp} = (d_{1,r}^{chp}\phi_{t,\max}^{chp} - \phi_{t,h}^{chp})e_{1,r}^{chp} \tag{18}$$

$$d_{2,r}^{chp} = (d_{2,r}^{chp}\phi_{t,\max}^{chp} - \phi_{t,h}^{chp})e_{2,r}^{chp} \tag{19}$$

All the coefficients of equations (18) and (19) are fixed, and their values are given in reference [48]. Also, the consumed natural gas amount by the CHP unit (F_t^{chp}) in the MEM can be calculated as follows [48]:

$$\mathrm{F}_t^{chp} = \frac{3.412}{GHV}\left(\frac{P_E^{chp} + \phi_t^{chp}}{\eta_t^{chp}}\right) \tag{20}$$

GHV_G is the amount of gross heat per unit volume of natural gas ($MBTU/m^3$) and η_t^{chp} is the CHP's overall efficiency. The gas consumption value by the gas-fired boiler (F_t^{Gcb}) unit to generate heat energy can be expressed as

follows [49]:

$$\mathrm{F}_{t}^{Gcb} = \frac{3.412}{GHV}(a^{boil}.(\phi_t^{Gcb})^2 + b^{boil}.\phi_t^{Gcb} + c^{boil}) \tag{21}$$

In this regard, ϕ_t^{Gcb} is the produced thermal power by the boiler. The maximum amount of thermal power that a boiler can generate is represented by $\phi_{t,max}^{Gcb}$. a^{Gcb} and b^{Gcb} express boiler partial loading constants. The electrical power amount used by the electric boiler (P_t^{Ecb}) can be evaluated by [50]:

$$P_t^{Ecb} = \frac{\phi_t^{Ecb}}{\eta_t^{Ecb}} \tag{22}$$

The amount of electric power consumption of the unit P2G (P_t^{P2G}) is determined as follows [51]:

$$\mathrm{P}_{t}^{P2G} = \frac{GHV_g}{\eta_t^{P2G}.3.412}.\mathrm{F}_{t}^{P2G} \tag{23}$$

The output thermal power of gas-fired and electric boilers should be between the minimum and maximum capacity of gas-fired and electric boilers, respectively:

$$\phi_{t,\min}^{Gcb} \le \phi_t^{Gcb} \le \phi_{t,\max}^{Gcb} \tag{24}$$

$$\phi_{t,\min}^{Ecb} \le \phi_t^{Ecb} \le \phi_{t,\max}^{Ecb} \tag{25}$$

The CHP's generated thermal power amount must be between the CHP's maximum and minimum values:

$$\phi_{t,\min}^{chp} \le \phi_{t,h}^{chp} \le \phi_{t,\max}^{chp} \tag{26}$$

The amount of generated natural gas by the P2G unit must be between the maximum and minimum generation values of the P2G unit, which is expressed according to the following relationship:

$$\mathrm{F}_{t,\min}^{P2G} \le \mathrm{F}_{t}^{P2G} \le \mathrm{F}_{t,\max}^{P2G} \tag{27}$$

The State Of Charge (SOC) of ESS ($P_{SOC,t}^{ESS}$) can be obtained by the following equation:

$$P_{SOC,t}^{ESS} = P_{SOC,t-1}^{ESS} + \eta_{ch}^{ESS} P_{ch,t}^{ESS} - \eta_{dch}^{ESS} P_{dch,t}^{ESS} \tag{28}$$

where η_{ch}^{ESS} and η_{dch}^{ESS} are charge and discharge efficiencies. In addition, the ESS cannot be charged and discharged simultaneously. Also, the rate of SOC changes related to the ESS should be considered as follows:

$$0 \le P_{ch,t}^{ESS} \le P_{ch,\max}^{ESS} \times \Delta t \tag{29}$$

$$0 \le P_{dch,t}^{ESS} \le P_{dch,\max}^{ESS} \times \Delta t \tag{30}$$

The upper/lower capacity limit for the ESS is as follows:

$$P_{SOC,\min}^{ESS} \le P_{SOC,t}^{ESS} \le P_{SOC,\max}^{ESS} \tag{31}$$

The AC unit's output cooling power is limited by the minimum $\left(\psi_{t,min}^{AC}\right)$ and maximum $\left(\psi_{t,max}^{AC}\right)$ capacities:

$$\psi_{t,\min}^{AC} \le \psi_{t}^{AC} \le \psi_{t,\max}^{AC} \tag{32}$$

In addition, the required heat energy for the AC unit (ϕ_t^{AC}) to produce cooling energy is calculated by the AC unit's efficiency ($\eta_{t,C}^{AC}$) as follows:

$$\phi_t^{AC} = \frac{\psi_{t,C}^{AC}}{\eta_{t,C}^{AC}} \tag{33}$$

The SOC related to TSS ($\phi_{SOC,t}^{TSS}$) is calculated considering the charge/discharge efficiency $\left(\eta_{ch}^{TSS}\right)$ /$\left(\eta_{dch}^{TSS}\right)$ as follows:

$$\phi_{SOC,t}^{TSS} = \phi_{SOC,t-1}^{TSS} + \eta_{ch}^{TSS}\phi_{ch,t}^{TSS} - \eta_{dch}^{TSS}\phi_{dch,t}^{TSS} \tag{34}$$

where $\phi_{ch/dch,t}^{TSS}$ is the charge/discharge value of TSS unit. The discharge and charge of each TSS cannot be simultaneously carried out. The lower/upper capacity limit and TSS charging/discharging ramp are represented by Eq. (35) and (36) – (37), respectively [52]:

$$\phi_{SOC,\min}^{TSS} \le \phi_{SOC,t}^{TSS} \le \phi_{SOC,\max}^{TSS} \tag{35}$$

$$0 \le \phi_{ch,t}^{TSS} \le \phi_{ch,\max}^{TSS} \times \Delta t \tag{36}$$

$$0 \le \phi_{dch,t}^{TSS} \le \phi_{dch,\max}^{TSS} \times \Delta t \tag{37}$$

The EC unit's cooling power is limited by its minimum $\left(\psi_{t,min}^{EC}\right)$ and the maximum $\left(\psi_{t,max}^{EC}\right)$ capacities as follows:

$$\psi_{t,\min}^{EC} \le \psi_{t,C}^{EC} \le \psi^{EC} \tag{38}$$

The electrical energy required for the EC unit (P_t^{EC}) to produce cooling can be expressed as follows:

$$P_t^{EC} = \frac{\psi_t^{EC}}{\eta_{t,C}^{EC}} \tag{39}$$

The SOC related to GSS ($F_{SOC,t}^{GSS}$) is calculated based on the following equation [53]:

$$\mathrm{F}_{SOC,t-1}^{GSS} = \mathrm{F}_{SOC,t-1}^{GSS} + \eta_{ch}^{GSS}\mathrm{F}_{ch,t}^{GSS} - \eta_{dch}^{GSS}\mathrm{F}_{dch,t}^{GSS} \tag{40}$$

where $F_{ch/dch,t}^{GSS}$ is the charge/discharge value of GSS unit. η_{ch}^{GSS} and η_{dch}^{GSS} are the charging and discharging efficiency of GSS, and GSS cannot be charged and discharged simultaneously. GSS capacity limits and the SOC ramp rate related to GSS are described by equations (41), (42), and (43), respectively:

$$\mathrm{F}_{SOC,\min}^{GSS} \le \mathrm{F}_{SOC,t}^{GSS} \le \mathrm{F}_{SOC,\max}^{GSS} \tag{41}$$

$$0 \le \mathrm{F}_{ch,t}^{GSS} \le \mathrm{F}_{ch,\max}^{GSS} \times \Delta t \tag{42}$$

$$0 \le \mathrm{F}_{dch,t}^{GSS} \le \mathrm{F}_{dch,\max}^{GSS} \times \Delta t \tag{43}$$

The SOC related to ISS ($\psi_{SOC,t}^{ISS}$) can be defined by considering the charge $\left(\eta_{ch}^{ISS}\right)$ and discharge $\left(\eta_{dch}^{ISS}\right)$ efficiencies using the following equations:

$$\psi_{SOC,t}^{ISS} = \psi_{SOC,t-1}^{ISS} + \eta_{ch}^{ISS}\psi_{ch,t}^{ISS} - \eta_{dch}^{ISS}\psi_{dch,t}^{ISS} \tag{44}$$

where $\psi_{ch/dch,t}^{CSS}$ is the charge/discharge value of ISS unit. The ISS cannot be simultaneously discharged and charged. In addition, the limits of ISS capacity and ramp rate for its SOC are expressed by equations (45) - (47), respectively:

$$\psi_{SOC,\min}^{ISS} \le \psi_{SOC,t}^{ISS} \le \psi_{SOC,\max}^{ISS} \tag{45}$$

$$0 \le \psi_{ch,t}^{ISS} \le \psi_{ch,\max}^{ISS} \times \Delta t \tag{46}$$

$$0 \le \psi_{dch,t}^{ISS} \le \psi_{dch,\max}^{ISS} \times \Delta t \tag{47}$$

The strategy adopted by the MEM operator and its decision-making parameters at every hour is expressed as follows:

$$X_t^{Hub} = (\phi_{ch,t}^{CSS}, \phi_{dch,t}^{CSS}, \phi_t^{chp}, \phi_t^{Gcb}, \phi_t^{Ecb}, \psi_{t,c}^{AC}, \psi_{dch,t}^{ISS}, \psi_{ch,t}^{ISS}, \psi_t^{EC}, \mathrm{F}_{ch,t}^{GSS}, \mathrm{F}_{dch,t}^{GSS}, \mathrm{F}_t^{P2G}, P_{dch,t}^{ESS}, P_{ch,t}^{ESS}, L_{e,out,DR}^t, L_{h,out,DR}^t) \tag{48}$$

4. Uncertainty Analysis of the MEM Based on the 2*m*+1 PEM

The existing uncertainties in the MEM operation may result in weak daily scheduling of the MEM. To overcome the MEM's uncertainties, this paper applies the point estimate method, which converts the stochastic daily MEM

scheduling problem into a 2*m*+1 equivalent deterministic daily MEM scheduling problem by specific weights. Suppose a function (F) that relates *m* input uncertain variables to an output uncertain variable (*S*) as follows [54]-[55].

$$S = F(z_1, z_2, ..., z_d, ..., z_m) \tag{49}$$

In Eq. (49), considering the optimal daily MEM scheduling problem, the variable *S* indicates the daily operating costs of the MEM, and function *F* is related to Eq. (1) with system constraints (6)-(47). Moreover, *m* represents the number of uncertain variables in the MEM system. In this regard, PEM replaces the PDFs of uncertain variables into three concentrated locations based on the Taylor series. Accordingly, each uncertain variable contains three concentration locations in the PEM with the *p*-th location $(z_{d,p})$, $p = 1,2,3$ and its weight factor ($\omega_{z,d}$) to evaluate the expected operation cost. The weighting factors reveal the corresponding location impact on the future expected operation cost of the integrated MEM. The following equations estimate the three concentration locations for uncertain variables, including generation power of wind and solar units, various energy demands, energy exchange prices, and their corresponding weight factors:

$$z_{d,p} = \mu_{z_d} + \xi_{z_{d,p}} \cdot \sigma_{z_d} \quad p = 1,2,3 \tag{50}$$

$$\xi_{z_{d,p}} = \frac{\lambda_{z_{d,3}}}{2} + (-1)^{3-p} \sqrt{\lambda_{z_{d,4}} - \frac{3}{4}\lambda^2_{z_{d,3}}} \quad for \;\; p = 1,2 \;\; \& \;\; \xi_{z_{d,3}} = 0 \tag{51}$$

$$\lambda_{z_{d,3}} = \frac{E\left[\left(z_d - \mu_{z_d}\right)^3\right]}{\left(\sigma_{z_d}\right)^3}, \quad \lambda_{z_{d,4}} = \frac{E\left[\left(z_d - \mu_{z_d}\right)^4\right]}{\left(\sigma_{z_d}\right)^4} \tag{52}$$

$$\omega_{z_{d,p}} = \frac{(-1)^{3-p}}{\xi_{z_{d,p}}\left(\xi_{z_{d,1}} - \xi_{z_{d,2}}\right)} \;\; p = 1,2 \;\; \& \;\; \omega_{z_{d,3}} = \frac{1}{m} - \frac{1}{\lambda_{z_{d,4}} - \lambda^2_{z_{d,3}}} \tag{53}$$

where, μ_{Z_d} is the mean value of an uncertain variable and σ_{Z_d} is the standard division value of it. $\xi_{Zd,P}$ is the standard location in PEM and $\lambda_{Z_{d,3}}$ and $\lambda_{Z_{d,4}}$, respectively, are the skewness and kurtosis of variable Z_d. After calculating concentration locations for uncertain parameters, the operation cost of the MEM should be evaluated for each concentration location. In this regard, one of the uncertain parameters in each hour, including various energy load demands, the wind power, the generated power by the solar unit, and energy exchange prices with upstream networks,

is fixed to its concentration location, and the other uncertain parameters are fixed to their mean values as follows:

$$Cost_{(d,p)} = F\left(\mu_{Z_1}, \mu_{Z_2}, ..., z_{d,p}, ..., \mu_{Z_m}\right) p = 1,2,3 \quad (54)$$

Based on the above equations, the expected operation cost of the energy MEM is calculated as follows:

$$Expected(\mathrm{Cos}t) = \sum_{d=1}^{m}\sum_{p=1}^{3}\omega_{z_{d,p}}.(\mathrm{Cos}(d,p)) = \sum_{d=1}^{m}\sum_{p=1}^{2}\omega_{z_{d,p}}.(\mathrm{Cos}(d,p)) + [F(\mu_{z1}, \mu_{z2}, ..., \mu_{zd}, ..., \mu_{zm})].\sum_{d=1}^{m}\omega_{zd,3} \quad (55)$$

5. Proposed Self-Adaptive Modified Slime Mould Algorithm

5.1. Original slime mould algorithm

The SMA has been adopted from the morphological changes and behaviour of slime mould Physarum polycephalum in foraging. In SMA, using three different morphotype weights, the negative and positive feedbacks of slime mould during foraging are simulated. The organic matter in slime mould looks for food and then surrounds it, and in the long run, secretes enzymes to digest food. During the migration process of slime mould, the front end extends into a fan-shaped, tracked by an interconnected venous network. The venous network allows cytoplasm to flow inside the network [42]. Since slime moulds have unique characteristics and patterns, they can surround different food sources simultaneously using the venous network. The mathematical modeling of slime mould mechanisms for the establishment of SMA is presented as follows [42]:

The SMA begins with a set of random agents called population, in which each agent is a candidate solution for optimizing the MEM scheduling problem [32]. Each agent is determined as follows:

$$Xi = [xi, 1xi, 2, ...xi, D] \quad i = 1, 2, ..., ps \quad (56)$$

where, D is the number of decision variables, and ps is the population size. The slime mould is approached to food based on the existence of odor in the air. Accordingly, the following equations describe the contraction mode and approach to a food of slime mould in SMA:

$$\overrightarrow{X^*} = \begin{cases} rand.(UB - LB) + LB, & rand < z \\ \overrightarrow{X_b(t)} + \overrightarrow{v_b} * (\overrightarrow{W}.\overrightarrow{X_A(t)} - \overrightarrow{X_B(t)}), & r < p \\ \overrightarrow{v_c}.\overrightarrow{X(t)}, & r \geq p \end{cases} \quad (57)$$

where $\overrightarrow{vc}$ is a parameter decreased linearly from one to zero. t is the current iteration, $\overrightarrow{X_i}$ is the new slime mould location, $\overrightarrow{X_b(t)}$ is the individual location that has the most odor concentration found by the algorithm, $\overrightarrow{X_A(t)}$ and $\overrightarrow{X_B(t)}$ represent two randomly selected locations. z is a setting parameter in SMA. r is a random variable between [0,1].

The following equations represent the other required parameters for the calculation of the new slime mould location:

$$p = \tanh|S(i) - DF| \qquad i \in 1,2,...,ps \tag{58}$$

where *S (i)* is the fitness value of *X* agent, and DF is the best fitness obtained in all iterations of SMA previously. $\overrightarrow{vb}$ is a random parameter located between [−a, a] and parameter a is calculated by:

$$a = \arctan h - t\max\_t + 1 \tag{59}$$

where *max_t* is the maximum iteration of SMA. *W* indicates the slime mould weight, which is represented as follows:

$$\overrightarrow{W(SmellIndex(l)} = \begin{cases} 1 + r.\log(\frac{bF - S(i)}{bF - wF} + 1), condition \\ 1 - r.\log(\frac{bF - S(i)}{bF - wF} + 1), \qquad other \end{cases} \tag{60}$$

$$SmellIndex = Sort(S) \tag{61}$$

The *condition* indicates whether *F(i)* is in the upper half of the sorted population or not. *bF* and *wF* denote the best and worst fitness values obtained in the current iteration. The *Sort* function arranges the solutions based on the most optimal objective function from top to bottom

5.2. Self-adaptive modified slime mould algorithm

The main goal of this self-adaptive modification is to compensate for the original SMA's shortcomings, and improve the SMA algorithm's convergence characteristics, and escape it from local optima. This self-adaptive modification is used to create diversity in different solution candidates' positions and prevent stagnation in the population. The original SMA is based on the two leading operators, including food search and approach to food. Hence, in the setting process between the food search and approach to food, the original SMA algorithm may fail to find global solutions and be trapped in local optima. The main reason for this mentioned issue is that the mutation operators in Eq. (57) for the original slim mould algorithm during the optimization process are inefficient and cannot

powerfully mutate the solution agents to reach the global optima. A new modification for the SMA solutions has been presented to enhance the SMA's ability and robustness. This mutation is derived from the wavelet theory [56], which is a potent tool for adequately adjusting the variables in each solution of the SMA algorithm, which increases its search potential. The name of this improved self-adaptive algorithm is SMSMA.

In this paper, to improve the performance of the SMA algorithm in essential exploration and exploitation procedures, the parameter $\vec{A}$ is created with a self-adaptive mechanism based on the wavelet theory. The parameter $\vec{A}$ based on the self-adaptive mechanism dynamically generates population mutations along the search path. The mathematic relations of the self-adaptive mechanism of the SMSMA algorithm are as follows:

$$\vec{A} = \frac{1}{\sqrt{h}} \exp^{\frac{-\left(\frac{\varphi}{h}\right)^2}{2}} \cos\left(5\left(\frac{\varphi}{h}\right)\right) \tag{62}$$

$$h = \exp^{-\ln(\eta)\times\left(1-iter/\mathrm{iter}_{\max}\right)^{\beta}+\ln(\eta)} \tag{63}$$

$$\beta = \beta_{\min} + \frac{\beta_{\max}-\beta_{\min}}{\mathrm{iter}_{\max}} \times iter \tag{64}$$

where η is the upper limit of h and β is the shape parameter of h. In this regard, a large value of $\vec{A}$ enlarges the search area and vice versa. Since 99% of the total Morlet wavelet energy is located in the interval [-2.5 - 2.5], φ can be chosen randomly in the interval [h*-2.5 - h*2.5]. In order to adapt the parameter $\vec{A}$ well, the value of the parameter (h) varies with time. In particular, in the initial iterations of the search, the value of h should be small and $\vec{A}$ should be large. In addition, with the increase of the iterations, the value of h should become larger, and the value of $\vec{A}$ should be decreased. Accordingly, in the initial stages, to have a small value of h, a small value of β should be applied. Hence, a wide-area search occurs in early iterations, and the search around the global optimal is encompassed later.

6. Numerical Results

This section investigates the efficiency of the proposed risk-based optimal scheduling framework on an integrated MEM system. The MEM system has been tested with two approaches. In the first approach, which is the primary and

deterministic state, the MEM performance is analyzed without considering the uncertainties of the system. In the following approach, the uncertainty effects of the renewable sources, the different types of loads, and the price of each energy carrier at the MEM's input are examined.

Table 2 shows the technical specifications of the MEM's internal equipment. The wind power unit is a turbine with 350 KW, and the solar power plant is a 700 KW unit. The structure of the proposed MEM is shown in Fig. 1. The distribution functions used for electrical and thermal load uncertainties are normal PDF [57]. Also, the energy price prediction errors [57], wind power [57], and photovoltaic power uncertainties [58] are modeled with normal PDFs. The standard deviation error of the uncertain variables is assumed to be 10%. The population and the maximum iterations in SMSMA are 50 and 200, respectively. To achieve the best minimization performance of MMSMA, the algorithm first has been run with the 200 population size and the 1000 maximum number of iterations. After that, the maximum number of the population and the iterations have been reduced with trial and error until the minimization of the MEM's operation cost is not changed. The results indicated that selecting populations and the maximum number of iterations for MMSMA to 50 and 200, respectively, could result in the best operation cost minimization performance and running time. Only 25% of the MEM's electrical, thermal, and cooling output loads are responsible. The proposed framework is solved by MATLAB software on a Core i7, 2.7 GHz PC with 4 GB RAM.

The price of each energy carrier at the input of the MEM is shown in Fig. 2. The amount of required electrical, cooling, and thermal loads at the MEM output over 24 hours are plotted in Fig. 3. The predicted daily power generation of the solar and the wind power units are demonstrated in Fig. 4.

The results of the daily scheduling of the MEM's internal equipment are shown in Fig. 5. It is evident from this figure that the MEM's CHP and boiler generate electricity only when the price of natural gas is low. In addition, the electric boiler in the system is not cost-effective for generating thermal energy. To produce cooling power, the AC

unit is economical equipment, and this device often works with maximum capacity at different hours. Also, the EC unit is used to provide the remaining cooling power. The energy storage units in the daily scheduling are frequently charged or discharged to reduce the MEM's total daily costs. The MEM operator generally tends to generate energy from the MEM's internal equipment rather than purchasing at high prices through upstream networks. The MEM operator buys the needed energy during the hours when the energy purchase prices are lower. This fact can be seen in the MEM's excess and deficiency power curves and the charge/discharge strategies of the MEM's storage units.

Fig. 6 shows the MEM's electric, gas, and thermal powers exchanging with the upstream networks. When the electricity demand is high between 10 am and 10 pm and the gas price is high, the MEM operator supplies its electricity demand by purchasing electricity from the upstream network. In addition, it is evident from this figure that when the gas price is low, the operator tends to buy gas energy, and when the gas price is high, the operator sells the MEM's surplus gas to the gas network. Moreover, when the gas price is high, the operator buys thermal energy to supply the MEM's heat demand. Also, the operator can sell the MEM's surplus thermal energy to the upstream heating network at other hours.

Table 3 indicates the comparison results of three uncertainty analysis methods to investigate the performance of the proposed *2m+1* PEM method. In this table, the MEM's daily operation costs for four uncertainty analysis methods, including the proposed *2m+1* PEM, *2m* PEM methods, Monte Carlo and the scenario-based method, have been presented. In this regard, it is notable that when the uncertainties are taken into account, the operating costs of the MEM are increased. Despite the increase in the MEM's operating costs in the 2*m*+1 point estimation method; this method is more effective because it provides a more realistic view of the system for the MEM operator. In addition, this table shows that the MEM's expected operating costs of the proposed *2m+1* PEM are very close to the Monte Carlo result. However, the running time of the proposed *2m+1* PEM is much lower than the Monte Carlo which indicates the superiority of the proposed *2m+1* PEM.

Fig. 7 depicts the tradeoff between CVaR and the expected operating costs of the MEM for various values of γ in

order to explore the effects of risk level on the MEM operation. As the level of the MEM's risk aversion increases, it is expected that the corresponding CVaR values will increase, and the MEM's expected operating costs will rise. The numerical outcomes shown in Fig. 7 support this fact.

To demonstrate the sensitivity of the total operation costs concerning the responsibility of loads and the increase in various storage capacities, Figures 8 and 9 are presented. As we can see from Figure 8, increasing the responsibility of loads to 20% results in a significant reduction in total operation costs. By increasing the responsibility of loads from 20%, the reduction in total operational costs is gradual. Moreover, Figure 9 indicates that increasing the various storage capacities by 40% can effectively reduce the total operational cost.

The comparative results between different optimization algorithms are presented in Table 4 in terms of statistical comparison indicators such as standard deviation, average, worst, and best solutions. It is noteworthy that the best result for each index in this table is typed in bold. Statistical indices show that the SMSMA algorithm is better than other well-known algorithms in all indices. The low standard deviation of the SMSMA algorithm compared to other algorithms shows the superiority of the proposed wavelet-based self-adaptive mutation to the original SMA algorithm. In this regard, in the wavelet theory, when the number of sample generations is significant, and samples are randomly generated in each iteration, it causes the sum of positive values of $\vec{A}$ and the sum of the negative values of $\vec{A}$ to be equal. Therefore, this feature of the proposed self-adaptive wavelet mutation method makes SMSMA experience a low standard deviation value. Considering the low standard deviation value of SMSMA compared to other algorithms reveals the quality and robustness of the self-adaptive modified mutation method for the original SMA algorithm. These comparisons show the ability of the SMSMA to solve the daily optimal scheduling problem of the MEM.

7. Conclusions

This paper presented a risk-based scheduling framework for multi-carrier MEM systems, considering the impacts

of responsive cooling and thermal and electrical energy loads. The objective function of the study is to minimize the MEM's operating costs and the risk associated with it due to system uncertainties. The well-known CVaR approach and the fast 2m+1 PEM uncertainty analysis method were employed to handle the risk arising from the uncertainties of renewable energy sources, various energy demands as well as energy purchasing prices at the MEM input. The operating effects of the MEM's several internal equipment and different energy storage units, especially ice storage, were investigated. Moreover, to solve the non-linear risk-based scheduling problem of the MEM, the new self-adaptive modified optimization algorithm named SMSMA was introduced.

According to the obtained results, it can be concluded that the proposed scheduling framework can specify the energy generation of the MEM's internal equipment as well as energy-exchanging values with the upstream energy networks. The hub's optimal policy is different at different times of the day according to the energy purchasing prices at the MEM input and different energy needs. Based on the results of the MEM's energy exchanges with the upstream networks and also the storage units' charging and discharging strategies, the system operator has been able to buy energy from the upstream networks at different times when the prices of energy carriers are low. Moreover, the MEM operator could sell the MEM's surplus energy when the price of energy carriers is high to make a profit. The ISS performance increases the MEM's flexibility to exert more energy resources, reducing costs besides utilizing other energy storages. The ice can be stored inside the MEM for short-term operation or long-term planning of the energy MEM. Results showed that with the increase in the parameter γ, the CVaR values related to the MEM's operating cost are significant. The numerical results also indicated the ability and robustness of the SMSMA algorithm to obtain the optimal solution of the risk-based daily scheduling problem of an integrated MEM compared to other algorithms.

Acknowledgment

H. R. Massrur wish to thank the Iran National Science Foundation for supporting this research.

Data availability

The data that supports the findings of this study are available within the article.

References

[1] Luo, J. Li, H. and Wang, Sh. “A quantitative reliability assessment and risk quantification method for microgrids considering supply and demand uncertaintie”, *Applied Energy*, 328, (2022). https://doi.org/10.1016/j.apenergy.2022.120130

[2] Esmaeili-Shayan, M. Najafi, G. Ghobadian, B. and et al. “Sustainable Design of a Near-Zero-Emissions Building Assisted by a Smart Hybrid Renewable Microgrid”, *International Journal of Renewable Energy Development*, 11(2), pp. 471-480 (2022). https://doi.org/10.14710/ijred.2022.43838

[3] Esmaeili-Shayan, M., Najafi, G., and Lorenzini, G. “Optimization of a dual fuel engine based on multi-criteria decision-making methods”, *Thermal Science and Engineering Progress*, 44, 102055, (2023). https://doi.org/10.1016/j.tsep.2023.102055

[4] Luo, J. Li, H. and Wang, Sh. “A quantitative reliability assessment and risk quantification method for microgrids considering supply and demand uncertaintie”, *Applied Energy*, 328, (2022). https://doi.org/10.1016/j.apenergy.2022.120130

[5] Liu, N. Tan, L. Sun, H. and et al. “Bilevel Heat–Electricity Energy Sharing for Integrated Energy Systems With Energy Hubs and Prosumers”, *IEEE Trans. on Indust. Inform.*, 18(6), pp. 3754-3765 (2022). https://doi.org/10.1109/TII.2021.3112095

[6] https://www.eia.gov/todayinenergy/detail.php?id=36692.

[7] Zhao, B. Zhao, Z. Huang, M. and et al. “Model Predictive Control of Solar PV-Powered Ice-Storage Air-Conditioning System Considering Forecast Uncertainties”, *IEEE Trans. on Sustainable Energy*, 12(3), pp. 1672-1683 (2021). https://doi.org/10.1109/TSTE.2021.3061776

[8] Massrur, H.R. Niknam, T. and Fotuhi-Firuzabad, M. “Day-ahead energy management framework for a networked gas–heat–electricity microgrid”, *IET Gener. Transm. Distrib.*, 13(20), pp. 4617-4629 (2019). https://doi.org/10.1049/iet-gtd.2019.0686

[9] Esmaeili-Shayan, M. Najafi, G.H. Ghobadian, B. and et al. “Multi-microgrid optimization and energy management under boost voltage converter with Markov prediction chain and dynamic decision algorithm”, *Renewable Energy*, 201(2), pp. 179-189, (2022). https://doi.org/10.1016/j.renene.2022.11.006

[10] Xie, Y. Lin, S. Liang, W. and et al. “An Interval Probabilistic Energy Flow Calculation Method for CCHP Campus Microgrids”, *IEEE Systems Journal*, 16(4), (2022). https://doi.org/10.1109/JSYST.2022.3156383

[11] Moradi, M.H. Abedini, M. and Hosseinian, S.M. “Optimal operation of autonomous microgrid using HS–GA”, *Int. J. Electr. Power Energy Syst.*, 77, pp. 210-220 (2016). https://doi.org/10.1016/j.ijepes.2015.11.043

[12] Sharma, I. Dong, J. Malikopoulos, A. and et al. “A modeling framework for optimal energy management of a residential building”, *Energy Build.*, 130, pp. 55-63 (2016). https://doi.org/10.1016/j.enbuild.2016.08.009

[13] Geidl, M. and Andersson, G. “Optimal power flow of multiple energy carriers”, *IEEE Trans. Power Syst.*, 22(1), pp. 145-155 (2007). https://doi.org/10.1109/TPWRS.2006.888988

[14] Massrur, H.R. Niknam, T. Aghaei, J. and et al. “Fast decomposed energy flow in large-scale integrated electricity–gas–heat energy systems”, *IEEE Trans. Sustain. Energy*, 9(4), pp. 1565-1577 (2018). https://doi.org/10.1109/TSTE.2018.2795755

[15] Tian, L. Cheng, L. Guo, J. and et al. “System Modeling and Optimal Dispatching of Multi-energy Microgrid with Energy Storage”, *Journal of Modern Power Systems and Clean Energy*, 8(5), pp. 809-819 (2020). https://doi.org/10.35833/MPCE.2020.000118

[16] Liu, W. Li, P. Yang, W. and et al. “Optimal Energy Flow for Integrated Energy Systems Considering Gas Transients”, *IEEE Transactions on Power Systems*, 34(6), pp. 5076-5079 (2019). https://doi.org/10.1109/TPWRS.2019.2929685

[17] Ezzati, S.M. Faghihi, F. Mohammadnezhad-shourkaaei, H. and et al. “Optimum operation of multi-energy carriers in the context of an energy hub considering a wind generator based on linear programming”, *J. Renew. Sust. Energ*, 10(1), (2018). https://doi.org/10.1063/1.4991984

[18] El-Zonkoly, A.M. Abdelaziz, A.Y. and Eladl, A.M. “Double-layer Firefly Algorithm for Simultaneous Optimal Sizing and Operation of Energy Hubs”, *Elec. Power Components and Syst.*, 45(16), pp. 1846-1857 (2018). https://doi.org/10.1080/15325008.2017.1377318

[19] Najafi, A. Tavakoli, A. Pourakbari-Kasmaei, M. and et al. “A risk-based optimal self-scheduling of smart energy hub in the day-ahead and regulation markets”, *J. Clean. Prod.*, 279, (2021). https://doi.org/10.1016/j.jclepro.2020.123631

[20] Chehreghani-Bozchalui, M. Cañizares, C.A. and Bhattacharya, K. “Optimal Energy Management of Greenhouses in Smart Grids”, *IEEE Transactions on Smart Grid*, 6(2), pp. 827-835 (2015). https://doi.org/10.1109/TSG.2014.2372812

[21] Bahmani, M.H. Esmaeili-Shayan, M. and Fioriti, D. “Assessing electric vehicles behavior in power networks: A non-stationary discrete Markov chain approach”, *Electric Power Systems Research*, 229, 110106 (2024). https://doi.org/10.1016/j.epsr.2023.110106

[22] Neyestani, N. Yazdani-Damavandi, M. Shafie-Khah, M.R. and et al. “Stochastic Modeling of Multienergy Carriers Dependencies in Smart Local Networks With Distributed Energy Resources”, *IEEE Trans. on Smart Grid*, 6(4), pp. 1748-1762 (2015). https://doi.org/10.1109/TSG.2015.2423552

[23] Ghappani, A. and Karimi, A. “Optimal operation framework of an energy hub with combined heat, hydrogen, and power (CHHP) system based on ammonia”, *Energy*, 266, (2023). https://doi.org/10.1016/j.energy.2022.126407

[24] Niknam, T. and Massrur, H.R. “Stochastic mid-term generation scheduling incorporated with wind power”, *International Journal of Electrical Power & Energy Systems*, 64, pp. 937-946 (2015). https://doi.org/10.1016/j.ijepes.2014.07.076

[25] Massrur, H.R. Niknam, T. Aghaei, J. and et al. “A stochastic mid-term scheduling for integrated wind-thermal systems using self-adaptive optimization approach A comparative study”, *Energy*, 155, pp. 552-564 (2018). https://doi.org/10.1016/j.energy.2018.05.025

[26] Massrur, H.R. Niknam, T. Fotuhi-Firuzabad, M. and et al. “Hourly electricity and heat Demand Response in the OEF of the integrated electricity-heat-natural gas system”, *IET Renewable Power Generation*, 13, pp. 2853-2863 (2019). https://doi.org/10.1049/iet-rpg.2018.5859

[27] Rouhani, S.H. Mojallali, H. and Baghramian, A. “Accurate demand response participation in regulating power system frequency by Modified Active Disturbance Rejection Control*”, Math Meth Appl Sci*., 45(12), pp. 7685-7699 (2022). https://doi.org/10.1002/mma.8271

[28] Lu, X. Liu, Zh. Ma, L. and et al. “A robust optimization approach for optimal load dispatch of community energy hub”, *Apply Energy*, 259, (2020). https://doi.org/10.1016/j.apenergy.2019.114195

[29] Alipour, M. Zare, K. and Abapour, M. "MINLP Probabilistic Scheduling Model for Demand Response Programs Integrated Energy Hubs", *IEEE Transactions on Industrial Informatics*, 14(1), pp. 79-88 (2018). https://doi.org/10.1109/TII.2017.2730440

[30] Wang, Y. Zhang, N. Kang, C. and et al. "Standardized Matrix Modeling of Multiple Energy Systems", *IEEE Transactions on Smart Grid*, 10(1), pp. 257-270 (2019). https://doi.org/10.1109/TSG.2017.2737662

[31] Zhao, Z. Guo, J. Luo, X. and et al. "Distributed Robust Model Predictive Control-Based Energy Management Strategy for Islanded Multi-Microgrids Considering Uncertainty", *IEEE Trans. on Smart Grid*, 13(3), pp. 2107-2120 (2022). https://doi.org/10.1109/TSG.2022.3147370

[32] Rastegar, M. Fotuhi-F, M. Zareipour, H. and et al. "A Probabilistic Energy Management Scheme for Renewable-Based Residential Energy Hubs", *IEEE Trans. Smart Grid*, 8(5), pp. 2217-2227 (2017). https://doi.org/10.1109/TSG.2016.2518920

[33] Jadidbonab, M. Mohammadi-lvatloo, B. Marzband, M. and et al. "Short-Term Self-Scheduling of Virtual Energy Hub Plant Within Thermal Energy Market", *IEEE Transactions on Industrial Electronics*, 68(4), pp. 3124-3136 (2021). https://doi.org/10.1109/TIE.2020.2978707

[34] Ha, T. Xue, Y. Lin, K. and et al. "Optimal Operation of Energy Hub Based Micro-energy Network with Integration of Renewables and Energy Storages", *Journal of Modern Power Systems and Clean Energy*, 10(1), pp. 100-108 (2022). https://doi.org/10.35833/MPCE.2020.000186

[35] Esmaeili-Shayan M. Ghasemzadeh, F. and Rouhani, S.H., "Energy storage concentrates on solar air heaters with artificial S-shaped irregularity on the absorber plate", *Journal of Energy Storage*, 74, (2023), 109289. https://doi.org/10.1016/j.est.2023.109289

[36] Gao, X. Chan, K.W. Xia, Sh. and et al. "Bidding strategy for coordinated operation of wind power plants and NGG-P2G units in electricity market", *CSEE Journal of Power and Energy Systems*, 8(1), pp. 212-224 (2022). https://doi.org/10.17775/CSEEJPES.2020.06100

[37] Liu, L. Li, W.D. Shen, J. and et al. "Probabilistic Assessment of β for Thermal Unit Using Point Estimate Method Adopted to a Low-Order Primary Frequency Response Model", *IEEE Trans. on Power Syst*, 34(3), pp. 1931-1941 (2019). https://doi.org/10.1109/TPWRS.2018.2889905

[38] Ongsakul, W. and Dieu, V.N. "Artificial intelligence in power system optimization", *Crc Press*, (2013). https://doi.org/10.1201/b14906

[39] Lee, T.Y. "Operating schedule of battery energy storage system in a time-of-use rate industrial user with wind turbine generators: a multipass iteration particle swarm optimization approach", *IEEE Trans. Energy Convers.*, 22(3), pp. 774-782 (2007). https://doi.org/10.1109/TEC.2006.878239

[40] Pedrasa, M.A.A. Spooner, T.D. and MacGill, I.F. "Coordinated scheduling of residential distributed energy resources to optimize smart home energy services", *IEEE Trans. Smart Grid*, 1(2), pp. 134-143 (2010). https://doi.org/10.1109/TSG.2010.2053053

[41] Zhao, F. Si, J. and Wang, J. "Research on optimal schedule strategy for active distribution network using particle swarm optimization combined with bacterial foraging algorithm", *Int. J. Electr. Power Energy Syst.*, 78, pp. 637-646 (2016). https://doi.org/10.1016/j.ijepes.2015.11.112

[42] Zhang, H. Cao, Q. Gao, H. and et al. "Optimum design of a multi-form energy hub by applying particle swarm optimization", *Journal of Cleaner Production*, 260, (2020). https://doi.org/10.1016/j.jclepro.2020.121079

[43] Cai, Z. Xiong, Z. Wan, K. and et al. “Node Selecting Approach for Traffic Network Based on Artificial Slime Mold”, *IEEE Access*, 8, pp. 8436-8448 (2020). https://doi.org/10.1109/ACCESS.2020.2964002

[44] Li, S. Chen, H. Wang, M. and et al. “Slime mould algorithm: A new method for stochastic optimization”, *Future Gener. Comput. Syst.*, 111, pp. 300-323 (2020). https://doi.org/10.1016/j.future.2020.03.055

[45] Cao, Y. Wei, W. Wang, J. and et al. “Capacity planning of energy hub in multi-carrier energy networks: A data-driven robust stochastic programming approach”, *IEEE Trans. Sustain. Energy*, 11(1), pp. 3-14 (2020). https://doi.org/10.1109/TSTE.2018.2878230

[46] Elsir, M. T.Al-Awami, A. A.Antar M. and et al. “Risk-Based Operation Coordination of Water Desalination and Renewable-Rich Power Systems”, *IEEE Transactions on Power Systems*,38(2), (2022). https://doi.org/10.1109/TPWRS.2022.3174565

[47] Bahrami, S. and Sheikhi, A. “From Demand Response in Smart Grid Toward Integrated Demand Response in Smart Energy Hub”, *IEEE Transactions on Smart Grid*, 7(2), pp. 650-658 (2016). https://doi.org/10.1109/TSG.2015.2464374

[48] Savola, T. and Keppo, I. “Off-design simulation and mathematical modeling of small-scale CHP plants at part loads”, *Appl. Thermal Eng.*, 25(8-9), pp. 1219–1232 (2005). https://doi.org/10.1016/j.applthermaleng.2004.08.009

[49] Shabanpour-Haghighi, A. and Seifi, A.R. “An Integrated Steady-State Operation Assessment of Electrical, Natural Gas, and District Heating Networks”, *IEEE Trans. on Power Sys.*, 31(5), pp. 3636-3647 (2016). https://doi.org/10.1109/TPWRS.2015.2486819

[50] Holjevac, N. Capuder, T. Zhang, N. and et al. “Corrective receding horizon scheduling of flexible distributed multi-energy microgrids”, *Applied Energy*, 207, pp. 176-194 (2017). https://doi.org/10.1016/j.apenergy.2017.06.045

[51] Tao, Y. Qiu, J. Lai, S. and et al. “Integrated Electricity and Hydrogen Energy Sharing in Coupled Energy Systems”, *IEEE Transactions on Smart Grid*, 12(2), pp. 1149-1162 (2021). https://doi.org/10.1109/TSG.2020.3023716

[52] Wei, J. Zhang, Y. Wang, J. and et al. “Multi-period planning of multi-energy microgrid with multi-type uncertainties using chance constrained information gap decision method”, *Applied Energy*, 260, (2020). https://doi.org/10.1016/j.apenergy.2019.114188

[53] Ju, L. Tan, Q. Lin, H. and et al. “A two-stage optimal coordinated scheduling strategy for micro energy grid integrating intermittent renewable energy sources considering multi-energy flexible conversion”, *Energy*, 196, (2020). https://doi.org/10.1016/j.energy.2020.117078

[54] Gallego, L. F.Franco, J. G.Cordero, L. and et al. “A fast-specialized point estimate method for the probabilistic optimal power flow in distribution systems with renewable distributed generation”, *Int. J. Electr. Power Energy Syst.*, 131, (2021). https://doi.org/10.1016/j.ijepes.2021.107049

[55] Mohseni-Bonab, S.M. Rabiee, A. Mohammadi-Ivatloo, B. and et al. “A two-point estimate method for uncertainty modeling in multi-objective optimal reactive power dispatch problem”, *Int. J. Electr. Power Energy Syst.*, 75, pp. 194-204 (2016). https://doi.org/10.1016/j.ijepes.2015.08.009

[56] Gouri, M.S. and Siva, R.V. “Enhancement of multimedia security using random permutation with wavelet function”, *Comput. And Electr. Eng.*, 63, pp. 41-52 (2017). https://doi.org/10.1016/j.compeleceng.2017.09.014

[57] Clegg, S. and Mancarella, P. “Storing renewables in the gas network: modelling of power-to-gas seasonal storage flexibility in low-carbon power systems”, *IET Gener. Transm. Distrib.*, 10(3), pp. 566-575 (2016).https://doi.org/10.1049/iet-gtd.2015.0439

[58] Mihaylov, B. R.Betts, T. Pozza, A. and et al. “Uncertainty estimation of temperature coefficient measurements of PV modules”, *IEEE J. Photovolt.*, 6(6), pp. 1554-1563(2016). https://doi.org/10.1109/JPHOTOV.2016.2598259

[59] Ma, T. Pei, W. Xiao, H. and et al. “The energy management strategies based on dynamic energy pricing for community integrated energy system considering the interactions between suppliers and users”, *Energy*, 211, 118677, (2020). https://doi.org/10.1016/j.energy.2020.118677

Mohamad Emadi was born in Borujerd, Iran, in 1987. He received his B.Sc., M.Sc., degree in Electrical Engineering from Islamic Azad University (Borujerd branch), in 2010, 2014, respectively. He is currently pursuing a Ph.D. in Power Engineering at Khorramabad Azad University. His main research interests include power electronic, power system management, multi-carrier energy systems, power system operation and control.

Hamid Reza Massrur received the M.Sc. and Ph.D. degrees in Electrical Engineering from Shiraz University of Technology, Shiraz, Iran. He completed his first and second Postdoctoral Fellowships at the Department of Electrical Engineering, Sharif University of Technology, Tehran, Iran in 2021 and 2023, respectively. He is currently a Postdoctoral Fellow at the Institute for Convergence Science and Technology (ICST) at Sharif University of Technology, Iran. His main research interests include power system operation and economics, data transmission in

smart grids, multi-carrier energy systems, demand-side management, advanced machine learning and artificial intelligence.

Esmaeel Rokrok was born in Khorramabad, Iran, in 1972. He received his B.Sc., M.Sc., and Ph.D. degree in Electrical Engineering from Isfahan University of Technology, in 1985, 1997 and 2010, respectively. He is an associate professor in the Department of Electrical Engineering, Lorestan University. His major research interests lie in the area of power system control and dynamics, dispersed generation, microgrid and robust control.

Amin Samanfar was born in Khorramabad, Iran, in 1978. He received his B.Sc. degree in electronic engineering from Semnan University, Semnan, Iran in 2001 and his M.Sc. degree from Tarbiat Modares University, Tehran, Iran, in 2004. Also, he received his Ph.D. degree in Electrical Engineering from Lorestan University, Lorestan, Iran, in 2018. He is an assistant professor in the Department of Electrical Engineering, Khorramabad Branch of Islamic Azad University, Khorramabad, Iran. His major research interests lie in the area of micro-grids, power system control and dynamic and Flexible Ac Transmission Systems.

Table captions:

Table 1. Taxonomy of the proposed the proposed risk-based optimal decision-making compared to the state-of-the-art and the existing literature.

Table 2. Characteristics of the MEM's internal equipment.

Table 3. Total daily MEM's operation costs by various uncertainty analysis methods

Table 4. Comparison of the statistical results of the proposed SMSMA algorithm and other well-known algorithms to solve the optimal daily scheduling problem of the MEM.

Figure captions:

Fig. 1. Generalized schematic of the integrated MEM.

Fig. 2. Predicted daily prices of different energy carriers at the MEM input [59].

Fig. 3. Predicted daily thermal and electrical loads at the MEM output [8].

Fig. 4 Daily predicted generation power of the solar and wind power units.

Fig. 5. Optimal operating of the MEM's internal equipment, a) Electrical equipment, b) Thermal equipment, c) Cooling equipment, d) Gas equipment.

Fig. 6. Power exchange of the MEM with the upstream networks. a) Electric power, b) Gas, c) Thermal power.

Fig. 7. The MEM's expected operating costs --versus the CVaR for different values of the risk management parameter γ.

Fig. 8. The sensitivity analysis of the total operation costs versus responsibility of loads.

Fig. 9. The sensitivity analysis of the total operation costs versus increasing in the various storage capacities.

Table 1. Taxonomy of the proposed the proposed risk-based optimal decision-making compared to the state-of-the-art and the existing literature.

Ref.	Output Energy Loads	Component Consideration	Risk Consideration	Uncertainty Modelling	Demand Response	Non-Constant Efficiency and Partial Loads	Storages
[10]	Electrical	Wind Unit, Diesel Generator, Fuel Cell	✗	✗	✗	✗	ESS
[11]	Electrical, Thermal	PV, DG, HVAC	✗	✓	✓	✗	ESS
[16]	Electrical, Thermal	CHP, Boiler, Wind Unit	✗	✓	✗	✗	ESS, TSS
[17]	Electrical, Thermal,	CHP, Boiler, AC	✗	✗	✗	✗	✗

	Cooling						
[18]	Electrical, Thermal	CHP, Boiler, Diesel Generator, Wind Unit	✓	✓	×	✓	ESS
[23]	Electrical, Thermal	CHP, Boiler, PV, Wind Unit	×	✓	✓	×	TSS
[28]	Electrical, Thermal	CHP, Boiler	×	✓	✓	×	ESS, TSS
[32]	Electrical, Thermal	CHP, Boiler, EB, Wind Unit	✓	✓	×	×	ESS, TSS
[33]	Electrical, Thermal, Cooling	CHP, GCB, PV, EC, AC, EB, Wind Unit	×	×	×	×	ESS, TSS, ISS
[34]	Electrical, Thermal	CHP, GCB, Wind Unit	×	✓	×	×	ESS
Proposed	Electrical, Thermal, Cooling	CHP, GCB, P2G, PV, EC, AC, EB, Wind Unit	✓	✓	✓	✓	ESS, TSS, GSS, ISS

Table 2. Characteristics of the MEM's internal equipment.

Equipment	**Technical Details**			
Electrical Boiler	$\phi_{t,max}^{Geb} = 500(KW)$		η =0.9	
Absorption Chiller	$\psi_{t,max}^{AC}$=1500 KW		η =0.85	
Electrical Chiller	$\psi_{t,max}^{EC}$ =1500 KW		η =0.6	
CHP	$\phi_{t,max}^{chp} = 1500(KW)$			
Gas-fired Boiler	$\phi_{t,max}^{Gcb} = 800(KW)$			
P2G	$\mathrm{F}_{\mathrm{t,max}}^{\mathrm{P2G}}$ =0.01 *(MSCM)*		η =0.7	
ESS	$P_{ch,max}^{ESS}$ =1000 KW	$P_{SOC,max}^{ESS}$=200 KW	$P_{SOC,max}^{ESS}$=300 KWh	$\eta_{c/d,ESS}$ =0.9
TSS	$\phi_{SOC,max}^{TSS}$ =1000 KW	$\phi_{dch,max}^{TSS}$ =200 KW	$\phi_{dch,Initial}^{TSS}$ =300 KWh	$\eta_{c/d,TSS}$ =0.9
GSS	$F_{SOC,max}^{GSS} = 0.01\ MSCM$	$F_{ch,max}^{GSS} = 0.003\ MSCM$	$F_{ch,Initial}^{GSS} = 0.003\ MSCM$	$\eta_{\frac{c}{d},GSS} = 1$
ISS	$\psi_{SOC,max}^{ISS} = 300(KW)$	$\psi_{\mathrm{dch,max}}^{\mathrm{ISS}} = 60(KW)$	$\psi_{\mathrm{dch},initial}^{\mathrm{ISS}} = 90(KWh)$	$\eta_{c/d,ISS} = 0.9$

Table 3. Total daily MEM's operation costs by various uncertainty analysis methods

Deterministic		Stochastic							
		Uncertainty Analysis Method							
		Monte Carlo		Scenario-Based		*2m* PEM		*2m+1* PEM	
		Expected	%SD	Expected	%SD	Expected	%SD	Expected	%SD
MEM's Operation Costs ($)	25737.4	25895.2	0.87	25914.3	1.42	25908.8	1.24	25897.7	1.02
Time (S)	5.41	1574		43		169		173	

Table 4. Comparison of the statistical results of the proposed SMSMA algorithm and other well-known algorithms to solve the optimal daily scheduling problem of the MEM.

Optimization algorithm	Operating cost ($)			
	Best	Average	Worst	Standard Deviation
GA	25848.6	25867.8	25893.5	3.537
PSO	25828.0	25846.1	25866.7	2.841
SMA	25784.6	25809.7	25839.3	1.274
SMSMA	**25737.4**	**25755.0**	**25779.4**	**0.341**

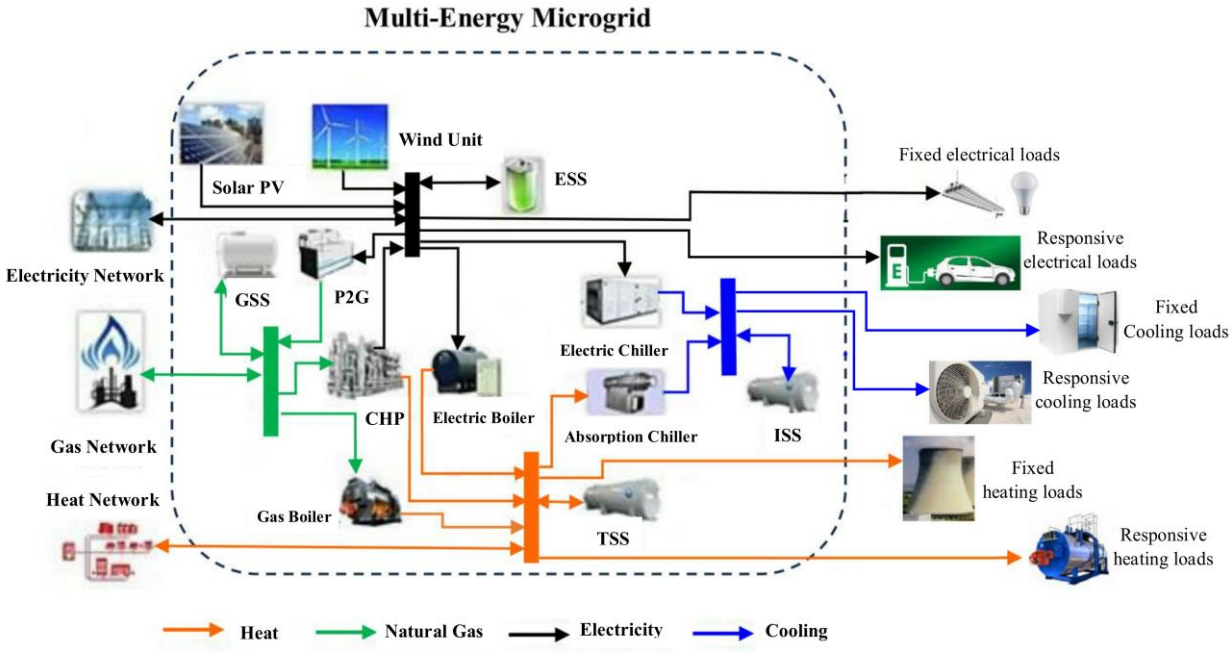

Fig. 1. Generalized schematic of the integrated MEM.

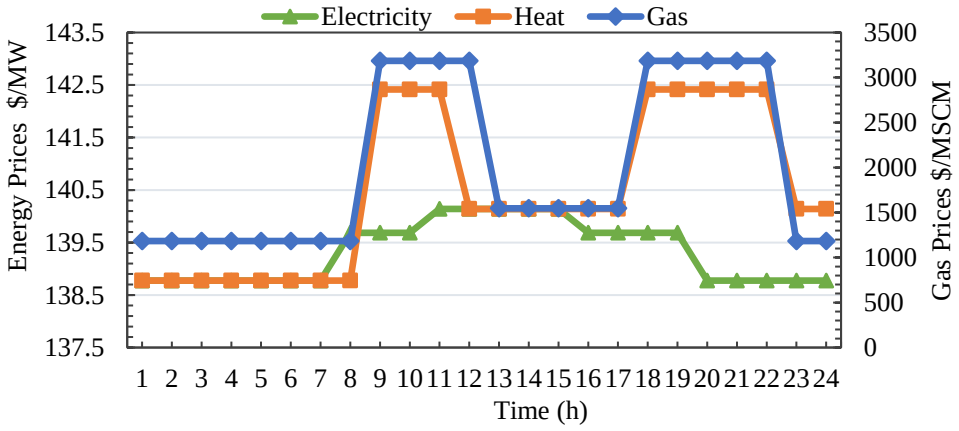

Fig. 2. Predicted daily prices of different energy carriers at the MEM input [59].

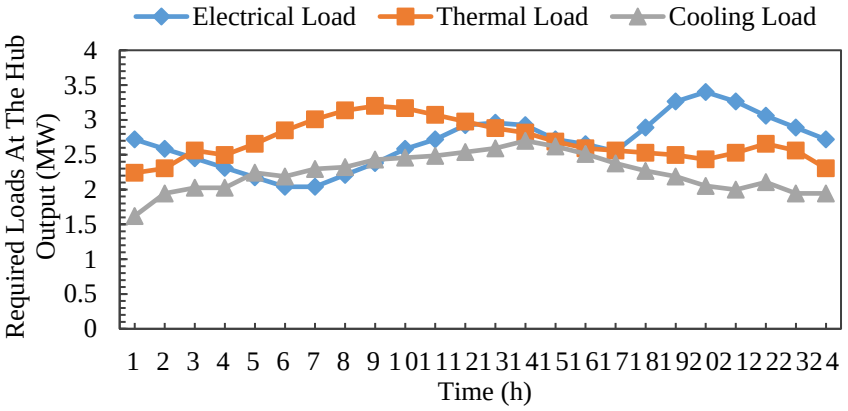

Fig. 3. Predicted daily thermal and electrical loads at the MEM output [8].

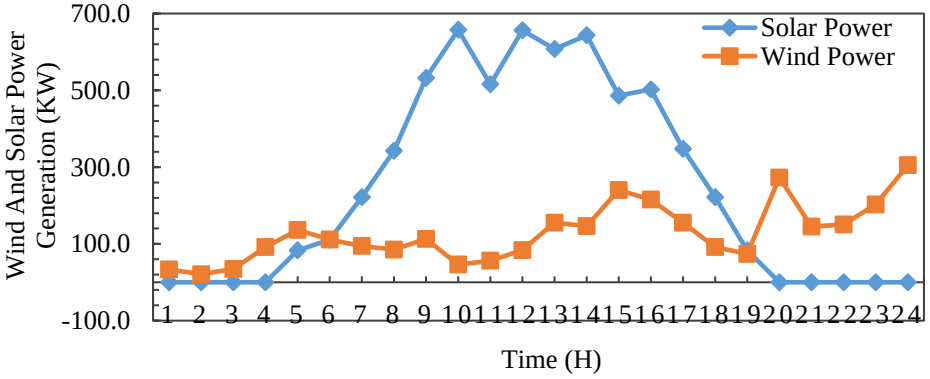

Fig. 4 Daily predicted generation power of the solar and wind power units.

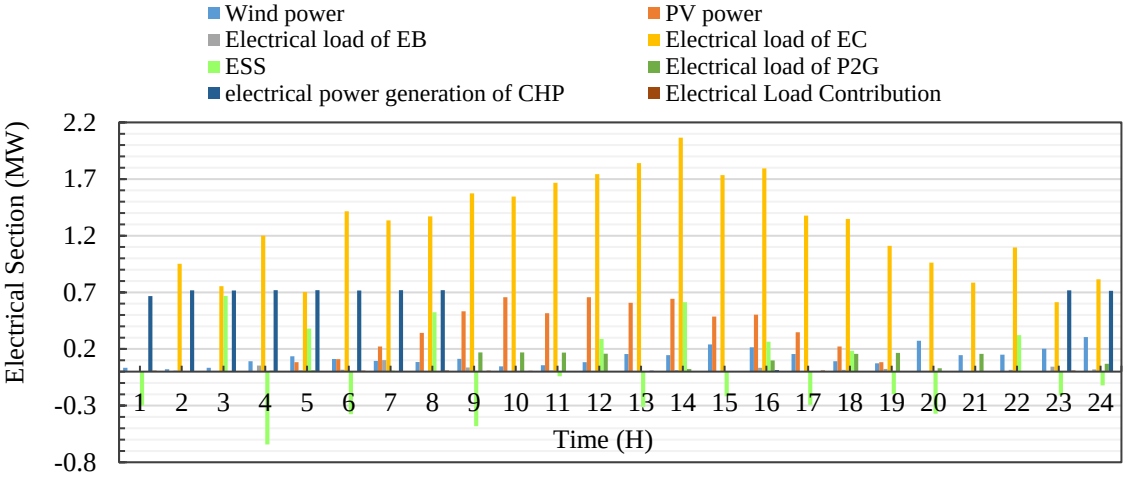
Wind power
PV power
Electrical load of EB
Electrical load of EC
ESS
Electrical load of P2G
electrical power generation of CHP
Electrical Load Contribution
Electrical Section (MW)
2.2
1.7
1.2
0.7
0.2
-0.3
-0.8
1 2 3 4 5 6 7 8 9 10 11 12 13 14 15 16 17 18 19 20 21 22 23 24
Time (H)

a

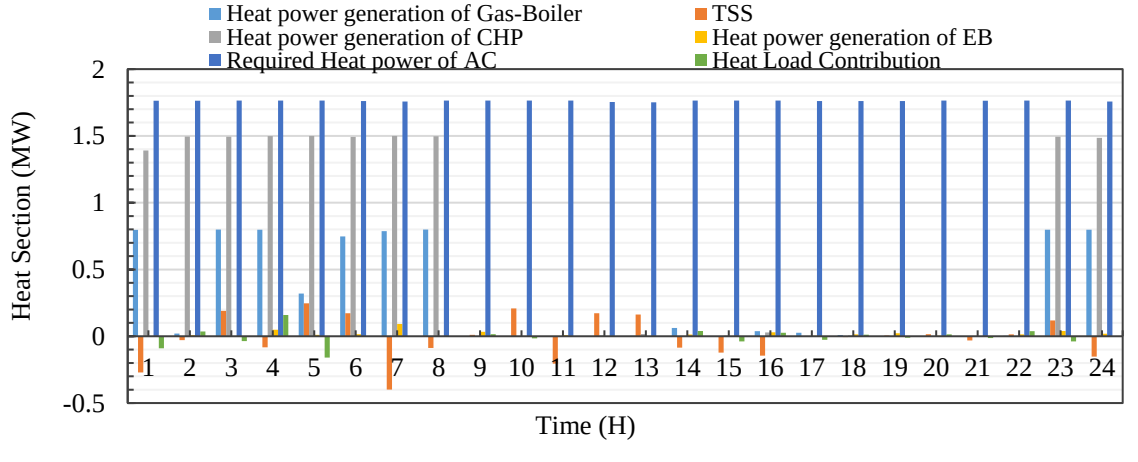
Heat power generation of Gas-Boiler
TSS
Heat power generation of CHP
Heat power generation of EB
Required Heat power of AC
Heat Load Contribution
Heat Section (MW)
2
1.5
1
0.5
0
-0.5
1 2 3 4 5 6 7 8 9 10 11 12 13 14 15 16 17 18 19 20 21 22 23 24
Time (H)

b

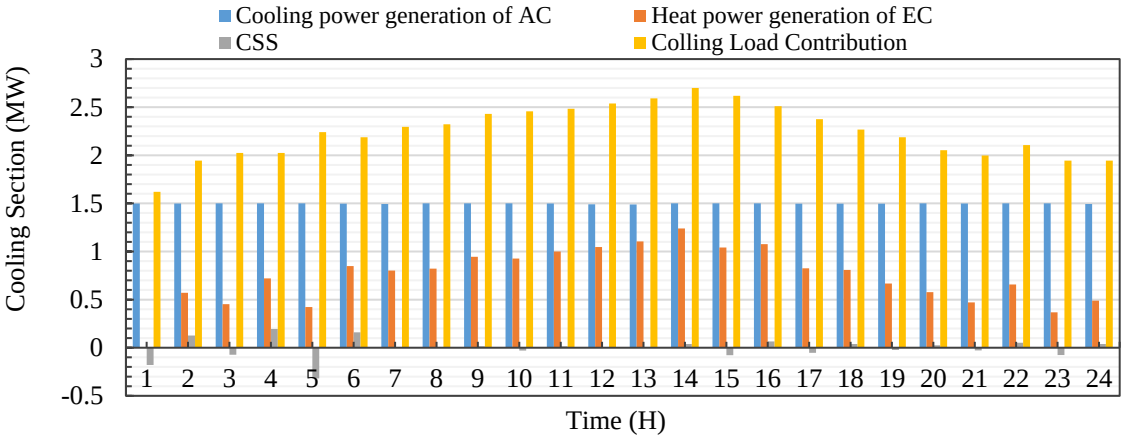

c

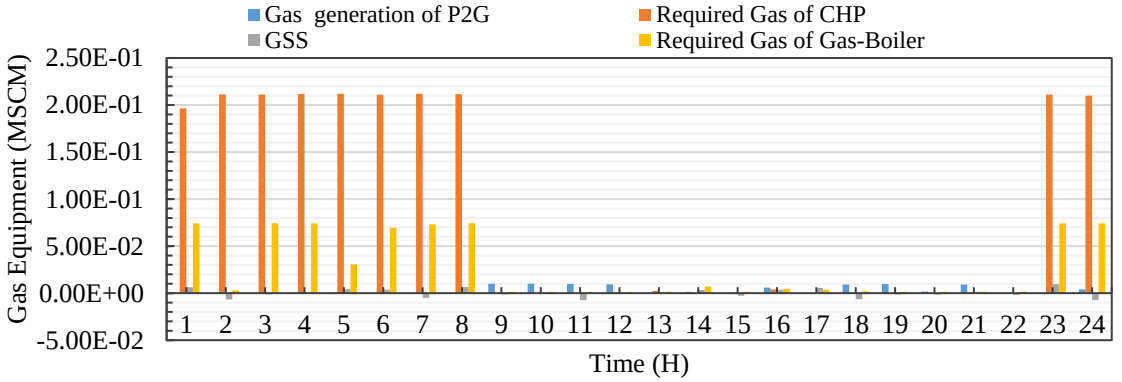

d

Fig. 5. Optimal operating of the MEM's internal equipment, a) Electrical equipment, b) Thermal equipment, c) Cooling equipment, d) Gas equipment.

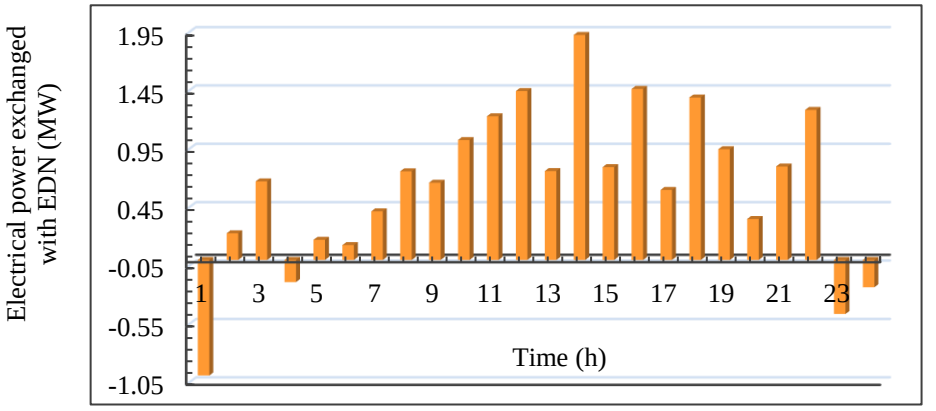
Electrical power exchanged with EDN (MW)
1.95
1.45
0.95
0.45
-0.05
-0.55
-1.05
1
3
5
7
9
11
13
15
17
19
21
23
Time (h)

a

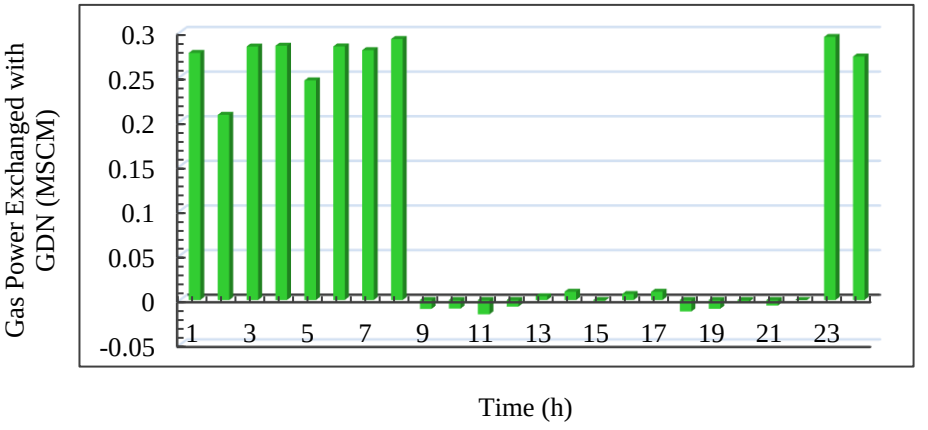
Gas Power Exchanged with GDN (MSCM)
0.3
0.25
0.2
0.15
0.1
0.05
0
-0.05
1
3
5
7
9
11
13
15
17
19
21
23
Time (h)

b

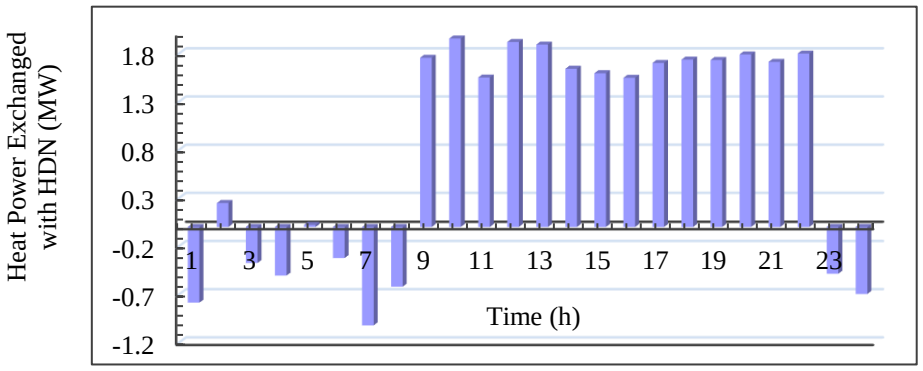

c

Fig. 6. Power exchange of the MEM with the upstream networks. a) Electric power, b) Gas, c) Thermal power.

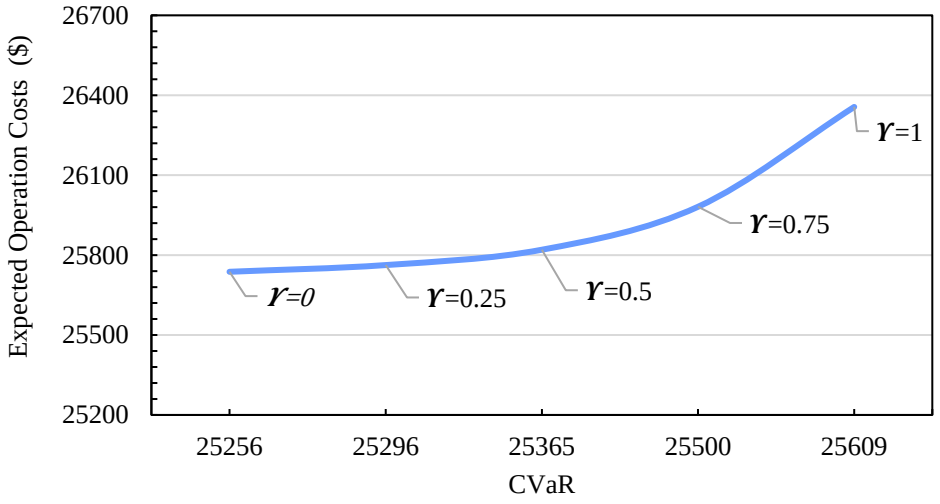

Fig. 7. The MEM's expected operating costs --versus the CVaR for different values of the risk management parameter γ.

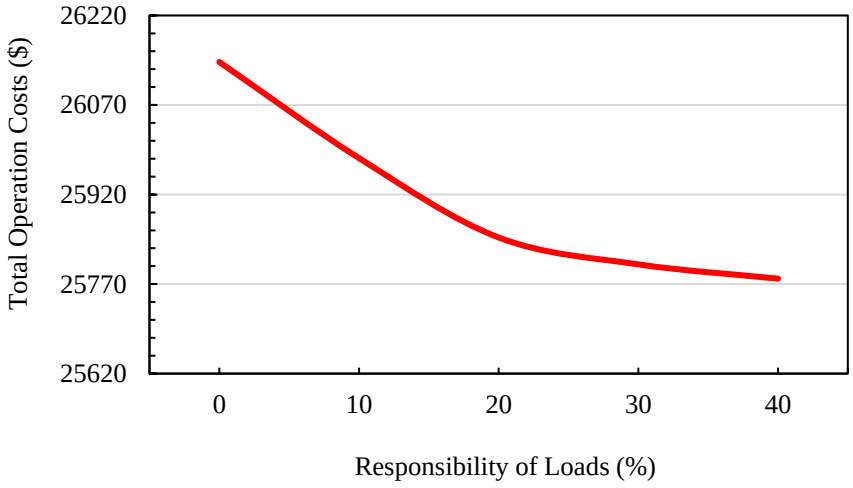

Fig. 8. The sensitivity analysis of the total operation costs versus responsibility of loads.

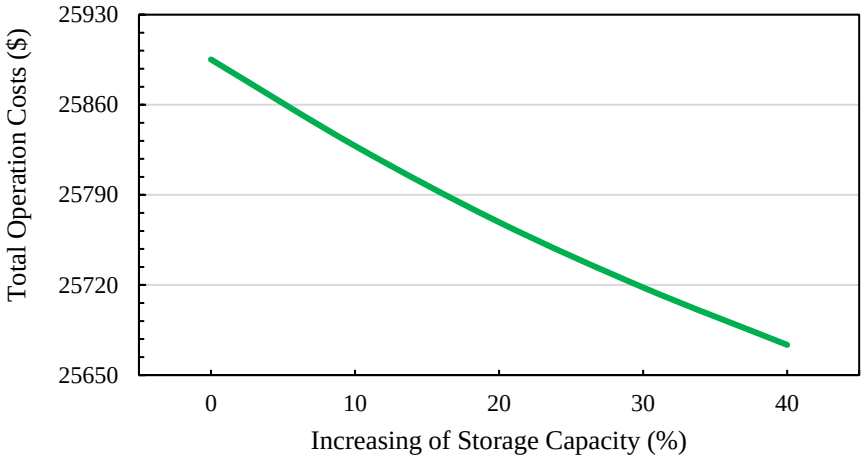

Fig. 9. The sensitivity analysis of the total operation costs versus increasing in the various storage capacities.